

Magic for the Age of Quantized DNNs

Yoshihide Sawada^{*1}, Ryuji Saiin^{*1,2}, and Kazuma Suetake²

¹Tokyo Research Center, AISIN, Tokyo, Japan

²AISIN SOFTWARE, Aichi, Japan

Abstract

Recently, the number of parameters in DNNs has explosively increased, as exemplified by LLMs (Large Language Models), making inference on small-scale computers more difficult. Model compression technology is, therefore, essential for integration into products. In this paper, we propose a method of quantization-aware training. We introduce a novel normalization (Layer-Batch Normalization) that is independent of the mini-batch size and does not require any additional computation cost during inference. Then, we quantize the weights by the scaled round-clip function with the weight standardization. We also quantize activation functions using the same function and apply surrogate gradients to train the model with both quantized weights and the quantized activation functions. We call this method *Magic for the age of Quantised DNNs (MaQD)*. Experimental results show that our quantization method can be achieved with minimal accuracy degradation.

1 Introduction

“

Any sufficiently advanced technology is indistinguishable from magic. ”

Arthur C. Clarke [6]

As computational power increases, the trend toward training large-scale deep neural networks (DNNs) on large-scale datasets continues unabated [5, 17, 31], and the use of cloud computing is essential for such large-scale DNNs. However, when real-time processing is required, such as in automatic driving peripheral recognition, online processing becomes difficult with the use of cloud computing. This implies that technology is required to integrate large-scale DNNs into small IoT devices, such as those based on microcontroller units [19, 20, 21]. Namely, model compression techniques, as in [13, 16, 22, 33], for integration into hardware will become more critical.

We are considering ways to quantize DNNs while training rather than quantizing the trained model, as we expect that the quantization-aware training has a better trade-off between compression efficiency and inference accuracy.

^{*}Equal contribution.

Preprint. Work in progress.

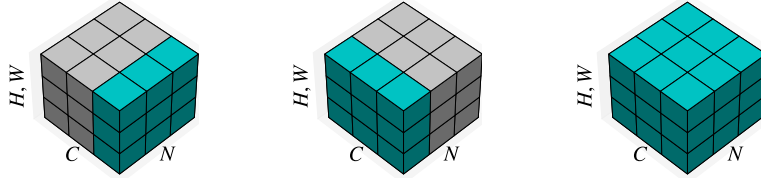


Figure 1: Range per normalization layer. Green areas are used for normalization, where C denotes the channel axis, N denotes the batch axes, and H and W denote the height and width axes, respectively. From left to right, BN, LN, and LBN are represented, respectively.

To achieve efficient quantization, we introduce a novel normalization technique called Layer-Batch Normalization (LBN), which is independent of the mini-batch size, unlike Batch Normalization (BN) [15]. LBN does not require computationally expensive expected value processes during inference for the normalization, unlike layer normalization (LN) [3]. In addition, because the proposed method is independent of the mini-batch size, we can train DNNs with smaller mini-batch sizes while maintaining accuracy. While BN recommends the use of large mini-batch sizes for training on large-scale datasets [29], which has resulted in an increased demand for machine resources, the proposed method can help alleviate this resource requirement. Figure 1 represents the overview of the LBN. On the basis of this normalization, weight standardization (WS) [26] and quantization by scaled round-clip functions and surrogate gradients [4, 7, 13, 30] can be combined to obtain the quantized DNNs with minimal accuracy degradation. We call this method *Magic for the age of Quantized DNNs (MaQD)*.

Our contributions of this study include the following:

- (1) We propose a novel normalization, LBN, which is independent of the mini-batch size and does not require computationally expensive expected value processes during inference.
- (2) We propose the MaQD, which combines the LBN, WS, scaled round-clip functions, and surrogate gradients, to train the quantized DNNs.
- (3) Experimental results show that our quantization technique achieves a good trade-off between compression efficiency and inference accuracy.

2 Preliminaries

In this section, we explain the traditional normalization [3, 15] and WS [26].

2.1 Normalization Layer

Let $a_{i,j,k}^{(l)} \in \mathbb{R}$ be the feature after weight transformation in the neural network, where $l \in \mathbb{N}$ represents the layer, $i \in \mathbb{N}$ ($1 \leq i \leq C^{(l)}$) represents the channel, $(j, k) \in \mathbb{N}^2$ ($1 \leq j \leq H^{(l)}, 1 \leq k \leq W^{(l)}$) represents the two-dimensional coordinates (because we consider the image classification tasks), and $C^{(l)}, W^{(l)}$,

and $H^{(l)}$ represent the channel, width, and height of the feature map in l -th layer. Then, the ordinary form of the normalization layer in the neural network, when $\mathbb{E}[\cdot]$ represents a certain expectation operator, is defined as follows:

$$\begin{aligned}\hat{a}_{i,j,k} &:= \frac{g_{i,j,k}}{\sigma_{i,j,k}}(a_{i,j,k} - \mu_{i,j,k}) + b_{i,j,k}, \\ \mu_{i,j,k} &:= \mathbb{E}[a_{i,j,k}], \\ \sigma_{i,j,k} &:= \sqrt{\mathbb{E}[(a_{i,j,k} - \mu_{i,j,k})^2] + \epsilon},\end{aligned}\tag{1}$$

where $g_{i,j,k}, b_{i,j,k} \in \mathbb{R}$ are the trainable parameters, and $\epsilon > 0$ is the constant to prevent divide-by-zero. Note that the normalization layer is applied to the features after the weight transformation and before the activation function, and the symbol (l) is removed for the simplicity. In addition, note that values can be pre-merged into other parameters (e.g., weights) if the $\mu_{i,j,k}$ and $\sigma_{i,j,k}$ are independent of input data during inference (i.e., in the case when the values can be fixed during inference).

2.1.1 Batch Normalization (BN) and Layer Normalization (LN)

In this section, we explain the LN [3] and BN [15], which are utilized by many DNNs, including Transformer [32], ResNet [10], and DenseNet [12]. The following equations represent the BN and LN, respectively.

$$\mathbb{E}_{\text{BN}}[z_{i,j,k}] := \frac{1}{HWN} \sum_{j=1}^H \sum_{k=1}^W \sum_{n=1}^N [z_{i,j,k}],\tag{2}$$

$$\mathbb{E}_{\text{LN}}[z_{i,j,k}] := \frac{1}{CHW} \sum_{i=1}^C \sum_{j=1}^H \sum_{k=1}^W [z_{i,j,k}],\tag{3}$$

where $z_{i,j,k} = z_{i,j,k}(\mathbf{x}_n)$ represents a function depending on a sample \mathbf{x}_n ($1 \leq n \leq N$) in the mini-batch. For the trainable parameters $g_{i,j,k}$ and $b_{i,j,k}$, the BN provides only channel dependence, whereas the LN provides both channel and coordinate dependence.

2.2 Weight Standardization (WS)

This section describes the standardization method for weights. Let $W_{\text{out,in}} \in \mathbb{R}$ denote the weight parameter. Then, the WS is denoted as follows [26]:

$$\begin{aligned}\hat{W}_{\text{out,in}} &:= \frac{W_{\text{out,in}} - \mu_{W_{\text{out}}}}{\sqrt{F_{\text{In}}\sigma_{W_{\text{out}}} + \epsilon}}, \\ \mu_{W_{\text{out}}} &:= \frac{1}{F_{\text{In}}} \sum_{\text{in}=1}^{F_{\text{In}}} W_{\text{out,in}}, \\ \sigma_{W_{\text{out}}} &:= \sqrt{\frac{1}{F_{\text{In}}} \sum_{\text{in}=1}^{F_{\text{In}}} (W_{\text{out,in}} - \mu_{W_{\text{out}}})^2},\end{aligned}\tag{4}$$

where F_{In} represents the number of fan-in.

3 Proposed Method

3.1 Layer-Batch Normalization (LBN)

The BN is a standard method for obtaining stable and good convergence results when training DNNs. However, to achieve this effect, ensuring a sufficiently large mini-batch size is necessary, which often requires a significant amount of memory capacity. On the other hand, the LN does not cause mini-batch dependence but does not provide the same training efficiency as the BN.

To complement these normalization layers, we propose the LBN as follows:

$$\mathbb{E}_{\text{LBN}}[z_{i,j,k}] := \frac{1}{CHWN} \sum_{i=1}^C \sum_{j=1}^H \sum_{k=1}^W \sum_{n=1}^N [z_{i,j,k}]. \quad (5)$$

Note that, for the trainable parameters $g_{i,j,k}$ and $b_{i,j,k}$, only the channel dependence is given, as in the BN.

3.2 Magic for the age of Quantized DNNs (MaQD)

This section explains the quantization of weights and activation functions. To quantize them, we use the following scaled round-clip function.

$$Q(z, \Delta, a, b) := \max \left(a, \min \left(b, \frac{\text{ROUND}(\Delta z)}{\Delta} \right) \right), \quad (6)$$

where $z \in \mathbb{R}$ represents the input to this function, $a, b \in \mathbb{R}$ represent the minimum and maximum values respectively, $\text{ROUND}(\cdot)$ represents the round function which outputs the integer nearest to the input, and $\Delta \in \mathbb{R}$ represents a value related to the number of states. Note that this function differs from [22] in that it includes Δ , which enables control over the degree of quantization.

Using Eq. 6, quantizations of the weights and activation functions are carried out as follows¹.

$$Q_w(\hat{W}_{\text{out,in}}, M_w) := Q \left(s\hat{W}_{\text{out,in}}, \frac{M_w}{2} \text{ or } \frac{M_w - 1}{2}, -1, 1 \right), \quad (7)$$

$$Q_a(\hat{a}_{i,j,k}, M_a) := Q(\hat{a}_{i,j,k}, M_a - 1, 0, 1), \quad (8)$$

where $M_w \in 2\mathbb{N} + 1$ and $M_a \in \mathbb{N}_{\geq 2}$. $s \in \mathbb{R}$ represents the scaling factor, and we set $s = 1/3$. This value gives a confidence interval of 99.7% if the distribution of weights corresponds to Gaussian. M_w and M_a represent the number of states for weights and activation functions, respectively. For example, if we quantize weights to 2 bits, we take values of $\{-1, 0, 1\}$ and set $M_w = 3$. This setting corresponds to 1.58 bits in [22]. Also, unlike quantization of weights, quantization of the activation function does not include values under zero. Namely, if we set 2 bits, $Q_a(\hat{a}_{i,j,k}, M_a)$ takes values of $\{0, 1/3, 2/3, 1\}$, and M_a becomes $4 = 2^2$. Note that we can achieve high computational efficiency and memory savings in such a quantized model by preparing additional floating scaling factors for each state during inference, as in [27].

¹We can select either $M_w/2$ or $(M_w - 1)/2$.

3.3 Training Process

In this article, we focus on the image classification tasks using the loss function L [28, 34] described as follows:

$$L := (1 - \gamma)\text{CE} + \gamma\text{MSE}, \quad (9)$$

where CE is the cross-entropy between the label and softmax output, and MSE is the mean-squared error between the one-hot encoded label and logit of softmax output. $\gamma \in \mathbb{R}$ is the hyperparameter to balance two losses and we set $\gamma = 0.05$. Note that while accuracy improvement through knowledge distillation [11, 24, 25] could easily be introduced to MaQD, we do not address this integration in this article as our focus is solely on the quantization itself.

To train models using the aforementioned loss function, differential calculations are necessary. However, MaQD is clearly non-differentiable. In this article, we adopt the surrogate gradient technique to approximate the gradient of the weights and activation functions as follows:

$$\frac{\partial Q_w(\hat{W}_{\text{out,in}}, M_w)}{\partial \hat{W}_{\text{out,in}}} := 1_{|s\hat{W}_{\text{out,in}}| < 1} (s\hat{W}_{\text{out,in}}), \quad (10)$$

$$\frac{\partial Q_a(\hat{a}_{i,j,k}, M_a)}{\partial \hat{a}_{i,j,k}} := \sum_{m=1}^{M_a-1} \frac{\partial \sigma_\alpha(\hat{a}_{i,j,k} - b_m)}{\partial \hat{a}_{i,j,k}}, \quad (11)$$

where $1_X(\cdot)$ denotes the indicator function on the set X , and $\partial \sigma_\alpha(\hat{z}_{i,j,k} - b_m) / \partial \hat{z}_{i,j,k}$ is the gradient of the scaled sigmoid function [30].

$$\frac{\partial \sigma_\alpha(z)}{\partial z} = \frac{1}{\alpha} \sigma_\alpha(z)(1 - \sigma_\alpha(z)), \quad (12)$$

$$\sigma_\alpha(z) := \frac{1}{1 + \exp(-z/\alpha)}. \quad (13)$$

Here, we set $\alpha = 0.25$. $b_m \in \mathbb{R}$ in Eq. 11 represents the threshold changing from m -th state to $(m + 1)$ -th state (e.g., the timing at which the output changes from 0 to 1 when we quantize to 1 bit), and the equation can be described as follows:

$$b_m = \frac{1}{\Delta} \left(\text{ROUND}_m(\Delta z) + \frac{1}{2} \right), \quad (14)$$

$$= \frac{1}{M_a - 1} \left((m - 1) + \frac{1}{2} \right), \quad (15)$$

where $m \in \mathbb{N}_{<M_a}$, and $\text{ROUND}_m(\cdot)$ denotes the m -th state (i.e., $\text{ROUND}_m(\cdot) := m - 1$). Figure 2 shows each surrogate gradient. Note that when the surrogate gradient of the activation function was set to Straight-Through Estimator (STE) [4, 7] as well as weights, the accuracy deteriorates significantly.

4 Experiments

We first demonstrate the effectiveness of the LBN (+WS) and then present the quantization results of the MaQD.

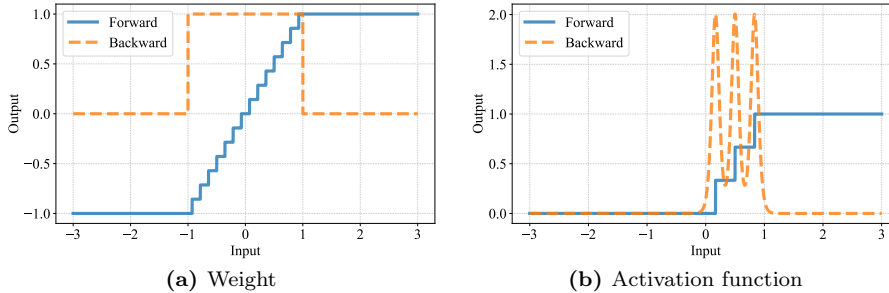


Figure 2: Surrogate gradients for weights and activation functions. The blue line represents forward propagation while the orange line represents backpropagation (surrogate gradient).

4.1 Verification of the Efficacy of LBN

In this section, we compare the normalization techniques, i.e., LBN+WS, LBN, BN+WS, and BN.

4.1.1 Settings

The following conditions were adopted to observe the differences between different normalizations when the mini-batch size varies:

- Dataset: CIFAR-100 [18]
- Network architecture: Non-quantized 9-layer CNN
- Hyperparameters:
 - Optimizer: Momentum SGD
 - Scheduler: Cosine Annealing
 - Learning rate, the number of epochs, and weight decay: The values obtained from the search with a mini-batch size of 128 were used as baseline values, and for the learning rate, the baseline values were multiplied by $N/128$ depending on the mini-batch size N . In particular, the total number of updates was automatically adjusted as the mini-batch size changed, while keeping the number of epochs constant.

4.1.2 Results

Figure 3 shows the experimental results. From the training results of each normalization method when varying the mini-batch size (Fig. 3, left), the following can be observed:

- LBN+WS achieves lower training losses than any of the other methods, regardless of the mini-batch size.
- LBN+WS exhibits less dependence on mini-batch size compared to BN, and loss difference between LBN+WS and BN diminishes as the mini-batch size increases.

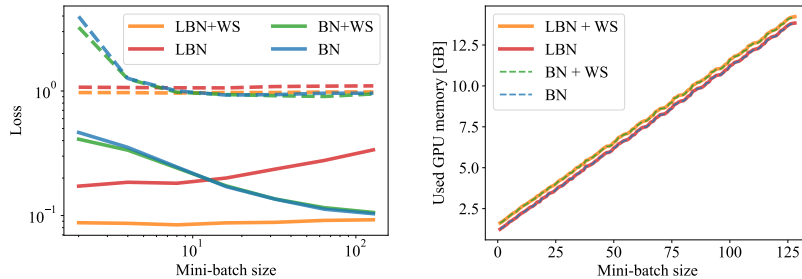


Figure 3: Left: Losses for training with varying mini-batch sizes for each normalization method. The solid and dashed lines represent the loss for the training and test datasets, respectively. Right: GPU memory usage when the mini-batch size is varied for each normalization method.

Next, from the GPU memory usage during training for each normalization when varying the mini-batch size (Fig. 3, right), the following can be observed:

- GPU memory usage increases in proportion to the mini-batch size.
- GPU memory usage varies among the methods, with the order being $BN < LBN < BN+WS < LBN+WS$ (although it may be difficult to discern from the figure, LBN uses slightly more GPU memory than BN).

These experimental results indicate that incorporating WS into BN does not enhance the independence of mini-batch size and that LBN without WS does not effectively reduce training and test losses. Therefore, it is crucial to utilize both WS and LBN in conjunction. Also, the impact on GPU memory usage is primarily determined by the mini-batch size rather than the choice of the normalization. Therefore, since LBN is independent of the mini-batch size, we require less GPU memory than existing methods while achieving low training and test losses (although LBN utilizes slightly more GPU memory than BN).

4.2 Verification of the Efficacy of MaQD

As described above, the LBN+WS provides better results than BN, especially when we set a small mini-batch size. Thus, this section shows the quantization results using LBN+WS (i.e., MaQD).

4.2.1 Settings

The following conditions were adopted to observe the differences between different normalizations when varying the mini-batch size:

- Dataset: CIFAR-10 [18] and CIFAR-100
- Network architecture: VGG and PreActResNet (see Appendix for details)
- Hyperparameters:
 - $M_w/2$ or $(M_w - 1)/2$ in Eq. 7: $M_w/2$
 - Optimizer: Momentum SGD
 - Scheduler: Cosine Annealing

Table 1: Performance with respect to varying M_w and M_a . The dataset is CIFAR-10, and the network architecture is VGG.

M_w	M_a	Accuracy [%]	R_w [%]	R_a [%]
Non-quantized		95.98	100	39.38
3	2	92.52	12.91	14.53
3	4	94.98	12.94	26.95
3	8	95.32	12.95	32.97
15	2	94.26	82.04	14.32
15	4	95.68	82.42	25.95
15	8	95.93	82.36	33.41
255	2	94.18	99.00	13.88
255	4	95.65	99.02	24.58
255	8	95.89	99.02	32.31

- Learning rate: 10^{-2}
- The number of epochs: 300
- Mini-batch size: 100

4.2.2 Results

Tables 1, 2, 3, and 4 and Figs. 4 and 5 show experimental results with respect to changing M_w and M_a . Here, R_w and R_a represent the ratio of non-zero parameters of weights and outputs of the activation functions, respectively. Note that for non-zero activation functions, we compute the value by averaging the non-zero ratio for each test sample. Also note that when $M_a = 2$, the model becomes S³NNs (Single Step Spiking Neural Networks) [30]. In this case, the normalization layers can be completely removed during inference by merging them with the weights. In other words, inference can be done using only additive operations (details are discussed in [30]).

From these results, the following can be observed:

- Setting M_w and M_a to small values reduces accuracy.
- However, sometimes the value relationship is reversed (e.g., $M_w = 255$ and $M_a = 8$ v.s. $M_w = 15$ and $M_a = 8$ in Table 1). Especially, $M_w = 255$ and $M_a = \{4, 8\}$ in Table 4 outperforms the non-quantized DNN.
- If M_w is fixed and M_a increases, the value of R_w remains almost the same, while the value of R_a increases.
- Remarkably, if M_a is fixed and M_w increases, the value of R_w increases, while the value of R_a decreases (especially in layers close to the input).

These results demonstrate the effectiveness of MaQD, particularly with $M_w = 15$ and $M_a = 8$, the model can be trained with an accuracy degradation of less than 1%. This means that, instead of setting the activation functions to 8 bits as in BitNet b1.58 [22], 3 bits may be sufficient. Also, as mentioned above, when $M_a = 2$, only additive operations can be used for inference. In this case, if we can utilize neuromorphic chips like TrueNorth [2] or Loihi [8], we can take advantage of asynchronous processing and significantly reduce power consumption [30]. That is, the appropriate degrees for quantization should be determined while considering the hardware for inference.

Table 2: Performance with respect to varying M_w and M_a . The dataset is CIFAR-10, and the network architecture is PreActResNet.

M_w	M_a	Accuracy [%]	R_w [%]	R_a [%]
Non-quantized		95.64	100	38.02
3	2	93.28	12.39	13.75
3	4	94.47	12.55	25.73
3	8	94.98	12.69	31.91
15	2	94.08	82.22	13.15
15	4	95.15	82.34	26.33
15	8	95.23	82.20	33.99
255	2	93.94	99.01	11.94
255	4	95.25	99.02	23.74
255	8	95.30	99.01	31.25

Table 3: Performance with respect to varying M_w and M_a . The dataset is CIFAR-100, and the network architecture is VGG.

M_w	M_a	Accuracy [%]	R_w [%]	R_a [%]
Non-quantized		76.52	100	40.89
3	2	69.19	12.51	17.35
3	4	74.02	12.64	32.45
3	8	74.85	12.71	38.54
15	2	72.27	82.78	17.10
15	4	75.44	82.58	29.23
15	8	75.66	82.49	36.33
255	2	72.73	99.04	16.75
255	4	76.08	99.03	27.51
255	8	75.86	99.03	34.47

Table 4: Performance with respect to varying M_w and M_a . The dataset is CIFAR-100, and the network architecture is PreActResNet.

M_w	M_a	Accuracy [%]	R_w [%]	R_a [%]
Non-quantized		75.47	100	37.89
3	2	70.23	12.32	15.71
3	4	73.68	12.63	29.20
3	8	74.31	12.71	34.83
15	2	71.29	82.58	15.67
15	4	75.28	82.39	28.82
15	8	75.26	82.33	34.55
255	2	72.54	99.03	13.68
255	4	75.48	99.02	24.48
255	8	75.91	99.02	31.78

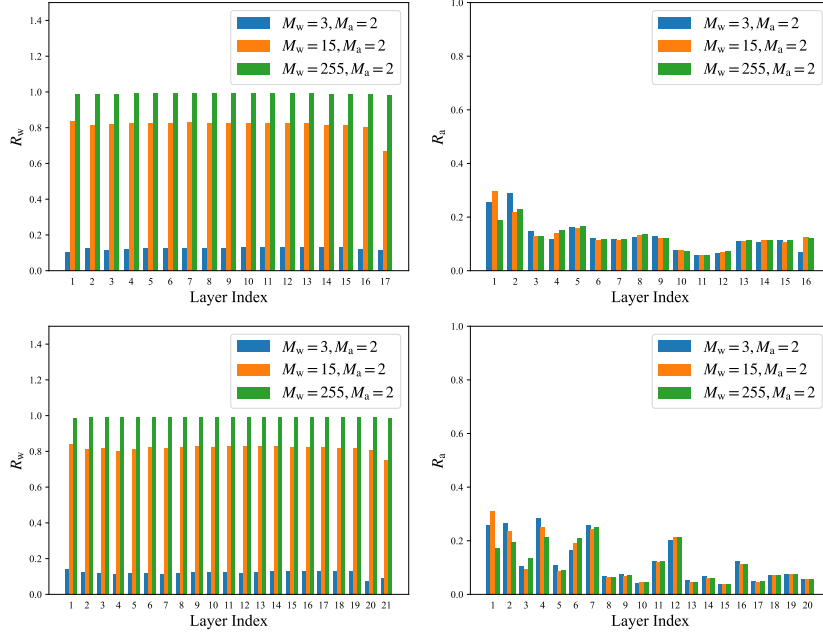


Figure 4: Examples of non-zero ratios for each layer when varying M_w and fixing M_a . The dataset is CIFAR-10, and the network architectures are VGG (top) and PreActResNet (bottom). Note that since the output layer is not quantized, the graph of R_a has one less layer index.

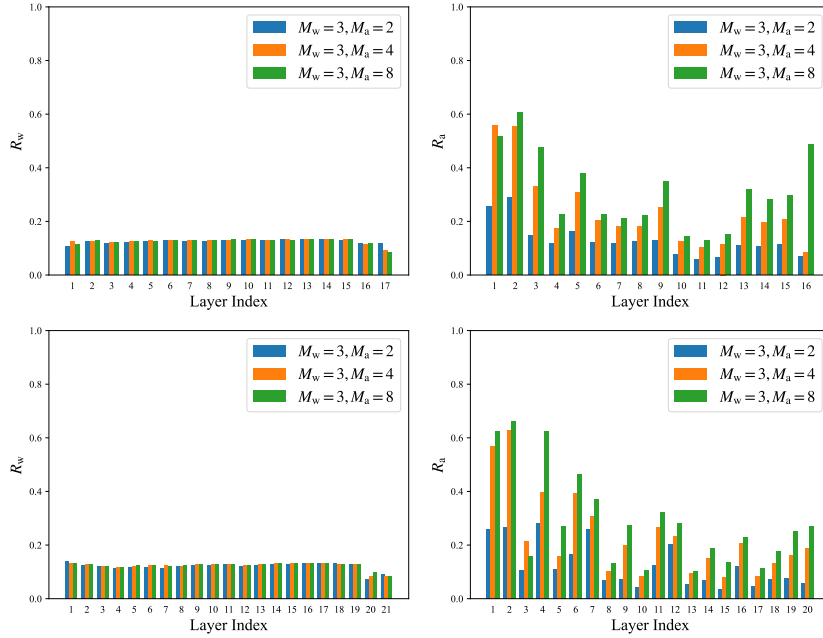


Figure 5: Examples of non-zero ratios for each layer when varying M_a and fixing M_w . The dataset is CIFAR-10, and the network architectures are VGG (top) and PreActResNet (bottom). Note that since the output layer is not quantized, the graph of R_a has one less layer index.

5 Conclusion

In this article, we proposed MaQD (Magic for the Age of Quantized DNNs) based on LBN (Layer-Batch Normalization), the scaled round-clip function, and the surrogate gradient. This enables model compression for product integration while reducing machine resource requirements by employing training with small mini-batch sizes. Applying this method to the image classification tasks, we confirmed its effectiveness.

In the future, the system will be demonstrated in challenging settings, such as the ImageNet dataset [9] and LLMs [5], which impose more demanding machine resource requirements, to showcase its versatility. It could also be a helpful combination with technologies like GaLore [35] and Evolutionary Model Merging [1], which have the potential to accelerate the democratization of AI development. Additionally, applications to SNNs (Spiking Neural Networks) [14, 23] that require time series processing will be explored.

We hope that *ubiquitous magic eventually becomes a gift to civilization.*

References

- [1] Akiba, T., Shing, M., Tang, Y., Sun, Q., Ha, D.: Evolutionary optimization of model merging recipes. arXiv preprint arXiv:2403.13187 (2024)
- [2] Akopyan, F., Sawada, J., Cassidy, A., Alvarez-Icaza, R., Arthur, J., Merolla, P., Imam, N., Nakamura, Y., Datta, P., Nam, G.J., et al.: Truenorth: Design and tool flow of a 65 mw 1 million neuron programmable neurosynaptic chip. IEEE transactions on computer-aided design of integrated circuits and systems **34**(10), 1537–1557 (2015)
- [3] Ba, J.L., Kiros, J.R., Hinton, G.E.: Layer normalization. arXiv preprint arXiv:1607.06450 (2016)
- [4] Bengio, Y., Léonard, N., Courville, A.: Estimating or propagating gradients through stochastic neurons for conditional computation. arXiv preprint arXiv:1308.3432 (2013)
- [5] Brown, T., Mann, B., Ryder, N., Subbiah, M., Kaplan, J.D., Dhariwal, P., Neelakantan, A., Shyam, P., Sastry, G., Askell, A., et al.: Language models are few-shot learners. Advances in neural information processing systems **33**, 1877–1901 (2020)
- [6] Clarke, A.C.: Hazards of prophecy: The failure of imagination. Profiles of the Future **6**(36), 1 (1962)
- [7] Courbariaux, M., Hubara, I., Soudry, D., El-Yaniv, R., Bengio, Y.: Binarized neural networks: Training deep neural networks with weights and activations constrained to+ 1 or-1. arXiv preprint arXiv:1602.02830 (2016)
- [8] Davies, M., Srinivasa, N., Lin, T.H., Chinya, G., Cao, Y., Choday, S.H., Dimou, G., Joshi, P., Imam, N., Jain, S., et al.: Loihi: A neuromorphic manycore processor with on-chip learning. Ieee Micro **38**(1), 82–99 (2018)

- [9] Deng, J., Dong, W., Socher, R., Li, L.J., Li, K., Fei-Fei, L.: Imagenet: A large-scale hierarchical image database. In: 2009 IEEE conference on computer vision and pattern recognition. pp. 248–255. Ieee (2009)
- [10] He, K., Zhang, X., Ren, S., Sun, J.: Deep residual learning for image recognition. In: Proceedings of the IEEE conference on computer vision and pattern recognition. pp. 770–778 (2016)
- [11] Hinton, G., Vinyals, O., Dean, J.: Distilling the knowledge in a neural network. arXiv preprint arXiv:1503.02531 (2015)
- [12] Huang, G., Liu, Z., Van Der Maaten, L., Weinberger, K.Q.: Densely connected convolutional networks. In: Proceedings of the IEEE conference on computer vision and pattern recognition. pp. 4700–4708 (2017)
- [13] Hubara, I., Courbariaux, M., Soudry, D., El-Yaniv, R., Bengio, Y.: Quantized neural networks: Training neural networks with low precision weights and activations. *Journal of Machine Learning Research* **18**(187), 1–30 (2018)
- [14] Ikegawa, S., Saiin, R., Sawada, Y., Natori, N.: Rethinking the role of normalization and residual blocks for spiking neural networks. *Sensors* **22**(8), 2876 (2022)
- [15] Ioffe, S., Szegedy, C.: Batch normalization: Accelerating deep network training by reducing internal covariate shift. In: International conference on machine learning. pp. 448–456. pmlr (2015)
- [16] Jacob, B., Kligys, S., Chen, B., Zhu, M., Tang, M., Howard, A., Adam, H., Kalenichenko, D.: Quantization and training of neural networks for efficient integer-arithmetic-only inference. In: Proceedings of the IEEE conference on computer vision and pattern recognition. pp. 2704–2713 (2018)
- [17] Kirillov, A., Mintun, E., Ravi, N., Mao, H., Rolland, C., Gustafson, L., Xiao, T., Whitehead, S., Berg, A.C., Lo, W.Y., et al.: Segment anything. In: Proceedings of the IEEE/CVF International Conference on Computer Vision. pp. 4015–4026 (2023)
- [18] Krizhevsky, A.: Learning multiple layers of features from tiny images. Master’s thesis, University of Tront (2009)
- [19] Lin, J., Chen, W.M., Cai, H., Gan, C., Han, S.: Memory-efficient patch-based inference for tiny deep learning. *Advances in Neural Information Processing Systems* **34**, 2346–2358 (2021)
- [20] Lin, J., Chen, W.M., Lin, Y., Gan, C., Han, S., et al.: Mcunet: Tiny deep learning on iot devices. *Advances in Neural Information Processing Systems* **33**, 11711–11722 (2020)
- [21] Lin, J., Zhu, L., Chen, W.M., Wang, W.C., Gan, C., Han, S.: On-device training under 256kb memory. *Advances in Neural Information Processing Systems* **35**, 22941–22954 (2022)

- [22] Ma, S., Wang, H., Ma, L., Wang, L., Wang, W., Huang, S., Dong, L., Wang, R., Xue, J., Wei, F.: The era of 1-bit LLMs: All large language models are in 1.58 bits. arXiv preprint arXiv:2402.17764 (2024)
- [23] Maass, W.: Networks of spiking neurons: the third generation of neural network models. *Neural networks* **10**(9), 1659–1671 (1997)
- [24] Okuno, T., Nakata, Y., Ishii, Y., Tsukizawa, S.: Lossless ai: Toward guaranteeing consistency between inferences before and after quantization via knowledge distillation. In: 2021 17th International Conference on Machine Vision and Applications (MVA). pp. 1–5. IEEE (2021)
- [25] Polino, A., Pascanu, R., Alistarh, D.: Model compression via distillation and quantization. In: International Conference on Learning Representations (2018)
- [26] Qiao, S., Wang, H., Liu, C., Shen, W., Yuille, A.: Micro-batch training with batch-channel normalization and weight standardization. arXiv preprint arXiv:1903.10520 (2019)
- [27] Rastegari, M., Ordonez, V., Redmon, J., Farhadi, A.: Xnor-net: Imagenet classification using binary convolutional neural networks. In: European conference on computer vision. pp. 525–542. Springer (2016)
- [28] Saiin, R., Shirakawa, T., Yoshihara, S., Sawada, Y., Kusumoto, H.: Spike accumulation forwarding for effective training of spiking neural networks. arXiv preprint arXiv:2310.02772 (2023)
- [29] Smith, S.L., Kindermans, P.J., Ying, C., Le, Q.V.: Don’t decay the learning rate, increase the batch size. In: International Conference on Learning Representations (2018)
- [30] Suetake, K., Ikegawa, S.i., Saiin, R., Sawada, Y.: S3NN: Time step reduction of spiking surrogate gradients for training energy efficient single-step spiking neural networks. *Neural Networks* **159**, 208–219 (2023)
- [31] Team, G., Anil, R., Borgeaud, S., Wu, Y., Alayrac, J.B., Yu, J., Soricut, R., Schalkwyk, J., Dai, A.M., Hauth, A., et al.: Gemini: a family of highly capable multimodal models. arXiv preprint arXiv:2312.11805 (2023)
- [32] Vaswani, A., Shazeer, N., Parmar, N., Uszkoreit, J., Jones, L., Gomez, A.N., Kaiser, L., Polosukhin, I.: Attention is all you need. *Advances in neural information processing systems* **30** (2017)
- [33] Wang, H., Ma, S., Dong, L., Huang, S., Wang, H., Ma, L., Yang, F., Wang, R., Wu, Y., Wei, F.: Bitnet: Scaling 1-bit transformers for large language models. arXiv preprint arXiv:2310.11453 (2023)
- [34] Xiao, M., Meng, Q., Zhang, Z., He, D., Lin, Z.: Online training through time for spiking neural networks. *Advances in Neural Information Processing Systems* **35**, 20717–20730 (2022)
- [35] Zhao, J., Zhang, Z., Chen, B., Wang, Z., Anandkumar, A., Tian, Y.: GaLore: Memory-efficient llm training by gradient low-rank projection. arXiv preprint arXiv:2403.03507 (2024)

A Network Details

In this paper, the VGG and PreActResNet used in the quantization experiments were set up as follows.

VGG: (64C3) \times 2-(128C3) \times 2-AP-(256C3) \times 4-AP-(512C3) \times 4-AP-(512C3) \times 4-10C1-GAP,
PreActResNet: 64B1-128B1-256B2-256B2-512B2-512B2-512B2-512B2-10C1-GAP,

where xCy represents the convolutional layer with x -output channels and y -stride, AP represents the average pooling with the kernel size 2, and GAP represents the global average pooling. Also, xBy represents the residual block,

$$xB_y := xS_y + xF_y, \quad (16)$$

where

$$\begin{aligned} xS_y &:= \text{LBN-ACT-}xCy\text{-LBN-ACT-}xCy\text{-LBN}, \\ xF_y &:= \text{LBN-ACT-}xCy\text{-LBN}, \end{aligned} \quad (17)$$

and ACT represents the (quantized) activation function. Note that the above description of VGG does not show the normalization layer for the simplicity, although the LBN is applied to the features after the weight transformation. The activation function (not shown above) is then utilized. Also, the PreActResNet performs AP before processing in blocks where the stride is set to 2 (although this is not explicitly specified too).